Autocrine production of IL-11 mediates tumorigenicity in hypoxic cancer cells

Barbara Onnis,[1] Nicole Fer,[2] Annamaria Rapisarda,[2] Victor S. Perez,[1] and Giovanni Melillo[2]

[1]Developmental Therapeutics Program and [2]SAIC-Frederick Inc., Frederick National Laboratory for Cancer Research, Frederick, Maryland, USA.

IL-11 and its receptor, IL-11Rα, are expressed in human cancers; however, the functional role of IL-11 in tumor progression is not known. We found that *IL11* is a hypoxia-inducible, VHL-regulated gene in human cancer cells and that expression of *IL11* mRNA was dependent, at least in part, on HIF-1. A cooperative interaction between HIF-1 and AP-1 mediated transcriptional activation of the *IL11* promoter. Additionally, we found that human cancer cells expressed a functional IL-11Rα subunit, which triggered signal transduction either by exogenous recombinant human IL-11 or by autocrine production of IL-11 in cells cultured under hypoxic conditions. Silencing of *IL11* dramatically abrogated the ability of hypoxia to increase anchorage-independent growth and significantly reduced tumor growth in xenograft models. Notably, these results were phenocopied by partial knockdown of *STAT1* in a human prostate cancer cell line (PC3), suggesting that this pathway may play an important role in mediating the effects of IL-11 under hypoxic conditions. In conclusion, these results identify *IL11* as an oxygen- and VHL-regulated gene and provide evidence of a pathway "hijacked" by hypoxic cancer cells that may contribute to tumor progression.

Introduction

Intratumoral hypoxia is a hallmark of human cancers. Changes in oxygen levels within solid tumors profoundly affect the behavior of cancer cells, contributing to resistance to radiation therapy and chemotherapy and ultimately to poor prognosis for patients (1, 2). Hypoxia triggers the angiogenic switch required for tumors to grow beyond a few cubic millimeters, shifts tumor metabolism to glycolysis for energy requirements, and increases the ability of cancer cells to invade and metastasize. In addition, hypoxia may select for cells resistant to apoptosis (3) and may induce genetic instability (4); however, the mechanism(s) by which hypoxia may contribute to tumorigenicity are still poorly understood. Notably, intratumoral hypoxia can also be exacerbated by vascular regression associated with anti-angiogenic therapy, which may cause a more chronic and pervasive decrease in oxygen levels, a phenomenon that has been implicated in the resistance to this therapeutic approach (5). A better understanding of signaling pathways that contribute to tumorigenicity of cancer cells in a hypoxic "stressed" tumor microenvironment is important for the identification of novel therapeutic targets and may lead to the development of more selective treatment strategies (6, 7).

The majority of the transcriptional responses to oxygen deprivation are mediated by hypoxia-inducible factor 1 (HIF-1), a heterodimeric transcription factor composed of a constitutively expressed β subunit and an oxygen-sensitive α subunit, of which 2 isoforms (HIF-1α and HIF-2α) have been best characterized in human cancers (8). The complex regulation of the HIF-α subunit, which in addition to oxygen levels is controlled by growth factors, cytokines, and genetic alterations frequently detected in human cancers, suggests that both hypoxic and nonhypoxic signaling pathways converge on HIF-1 to mediate the malignant phenotype. Indeed, HIF-1α overexpression is frequently observed in human cancers and is associated with poor patient prognosis in several tumor types, including breast, colon, lung, cervix, and head and neck (9–13).

IL-11 is a member of the IL-6 family of cytokines, which mediate signaling via a common signal-transducing gp130 component and a cytokine-specific subunit (14). Ligand binding to IL-11Rα triggers phosphorylation of associated JAK kinases. The activated JAK kinases recruit members of the STAT family of transcription factors (STAT3 and STAT1), which in turn undergo tyrosine phosphorylation, dimerization, and translocation to the nucleus, where they elicit activation of their target genes (14). Other signaling pathways that may be activated by IL-11 include the MAPKs, Src-family kinases, and PI3K pathway (15–17). The role of IL-11 in human pathophysiology is still poorly characterized. IL-11 was initially described as a hematopoietic cytokine with thrombopoietic activity and was subsequently found to be involved in pleiotropic effects on multiple tissues (18–20). Recently, IL-11 was implicated in experimental models of chronic inflammation and associated tumorigenesis, mediated at least in part by overactivation of STAT3 and STAT1 (21, 22). In addition, IL-11 expression is associated with poor survival in hepatocellular carcinoma (23) and has been associated with an aggressive phenotype and poor prognosis in gastric adenocarcinoma (24). Moreover, IL-11 has been shown to be expressed in metastasis of solid tumors (25), and it increases metastatic potential in breast cancer, endometrial carcinoma, and chondrosarcoma (26–28). However, whether and by what mechansim(s) IL-11 might contribute to tumor progression are not known.

We demonstrate here that *IL11* is a hypoxia-inducible gene in human cancer cells. Notably, autocrine production of IL-11 in hypoxic cancer cells triggered activation of oncogenic signaling pathways that contributed to increased tumorigenicity both in anchorage-independent growth and in xenograft models. These results provide evidence of a pathway "hijacked" by hypoxic cancer cells that may contribute to tumor progression, and they identify a potential novel target for cancer therapy.

Authorship note: Barbara Onnis, Nicole Fer, and Annamaria Rapisarda contributed equally to this work.

Conflict of interest: The authors have declared that no conflict of interest exists.

Citation for this article: *J Clin Invest.* 2013;123(4):1615–1629. doi:10.1172/JCI59623.

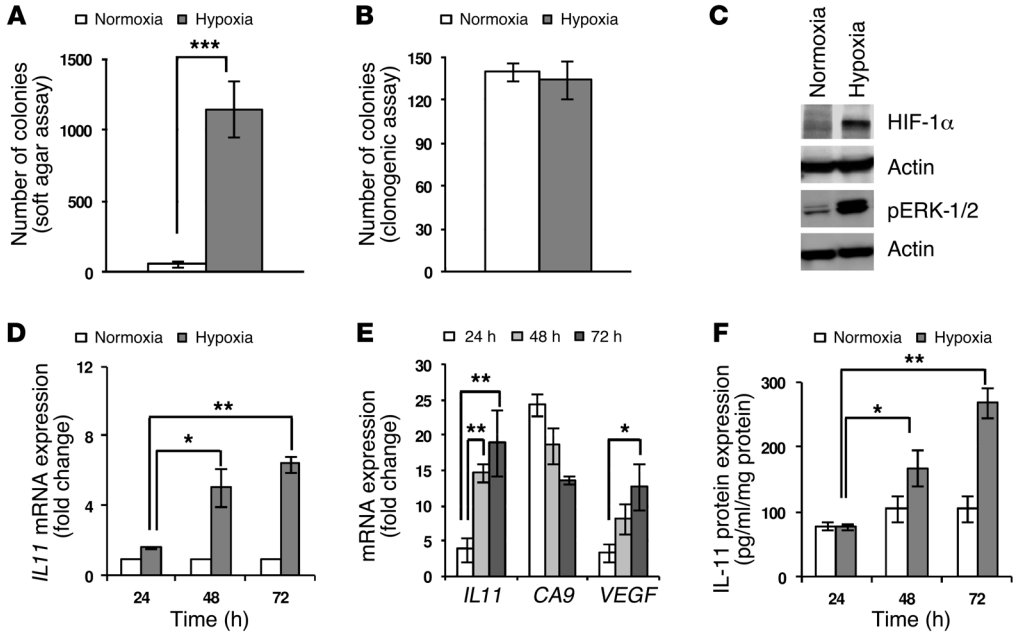

Figure 1

IL11 is a hypoxia-inducible gene. (**A**) HCT116 cells were serum starved for 24 hours, cultured under normoxia or hypoxia for an additional 72 hours, and then plated in soft agar (mean ± SEM of 3 independent experiments; *t* test). (**B**) HCT116 cells were cultured as described above and then plated for clonogenic assay. Colonies were stained after 10 days (mean ± SEM of 2 independent experiments). (**C**) Levels of ERK protein phosphorylation and HIF-1α protein were measured using Western blot analysis in HCT116 cells cultured as described above. Results are representative of 2 independent experiments. (**D**) HCT116 cells were cultured under normoxia or hypoxia for 24, 48, and 72 hours. *IL11* mRNA expression was analyzed using quantitative RT-PCR, and results are presented as the mean ± SEM of 2 independent experiments (*t* test). (**E**) PC3 cells were cultured under normoxia or hypoxia for 24, 48, and 72 hours. Results are presented as mean fold change relative to the normoxia sample ± SEM of 4 different quantitative RT-PCR experiments (*t* test). (**F**) Levels of IL-11 protein were measured in supernatant from PC3 cells cultured under normoxia or hypoxia for 24, 48, and 72 hours using a commercially available ELISA kit. Results represent the mean ± SEM of 3 separate experiments (*t* test). $^{*}P < 0.01$; $^{**}P < 0.001$; $^{***}P < 0.0001$.

Results

Hypoxia induces IL11 mRNA and protein expression. To identify novel signaling pathways that may contribute to tumorigenicity of cancer cells exposed to chronic hypoxic conditions, HCT116 human colon cancer cells were cultured under normoxic or hypoxic (1% O_2) conditions for 3 days (72 hours; Figure 1, A and B) or 5 days (120 hours; data not shown), at which point anchorage-independent growth, clonogenic survival on plastic, and protein expression were analyzed. HCT116 cells cultured for 72 hours under hypoxic conditions showed a significant advantage in colony formation under anchorage-independent conditions, but not on plastic, relative to normoxic cells (Figure 1, A and B), an indication that incubation under hypoxia did indeed increase tumorigenic potential of cancer cells. Moreover, HIF-1α protein and ERK phosphorylation were significantly increased in cells cultured under hypoxic conditions for 72 hours (Figure 1C), confirming that the experimental conditions used induced a hypoxic phenotype. Based on these preliminary results, we performed microarray analysis using Affymetrix arrays (HG-U133 Plus 2.0) in HCT116 cells cultured under normoxic or hypoxic conditions for 72 hours. Among the differentially regulated genes, we focused our attention on *IL11*, a gene that was expressed at higher levels in hypoxic cells and whose hypoxic inducibility was confirmed in a real-time PCR experiment with HCT116 that spanned over 72 hours (Figure 1D). These results provided the first evidence that *IL11* is a hypoxia-inducible gene. Additional real-time PCR experiments confirmed this pattern of expression in a number of different human cancer cell lines (Supplemental Figure 1; supplemental material available online with this article; doi:10.1172/JCI59623DS1). We demonstrated that *IL11* mRNA was induced by hypoxia in a time-dependent fashion (up to 11.1-fold relative to normoxic cells) in IGROV-1, NCI-H460, KM12, UACC62, and OVCAR-5 cells, with maximal induction at 72 hours (Supplemental Figure 1). More modest induction (<3-fold) was observed in HT29, MDA-MB231, and BT-549 cells (data not shown). The highest levels of hypoxic induction of *IL11* mRNA expression were observed in the PC3 prostate cancer cell line, which then became the focus of further investigation. As shown in Figure 1E, average levels of *IL11* mRNA expression in hypoxic PC3 cells were 3.3-, 14.6-, and 25.7-fold higher than those observed in normoxic cells at 24, 48, and 72 hours, respectively, confirming the trend observed in other cell lines of a time-dependent increase and maximal induction at 72 hours. We then analyzed the expression of 2 known HIF-1–dependent genes, *VEGF* and *CA9*. Interestingly, *VEGF* mRNA expression followed a similar trend of accumulation to IL-11 (Figure 1E), while mRNA levels of *CA9* were maximally induced at 24 hours in hypoxic PC3 cells and decreased over time (Figure 1E). Consistent with the induction of *IL11* mRNA expression, IL-11 protein was secreted by hypoxic PC3 cells in a time-dependent fashion, with up to 3-fold higher levels of IL-11 protein observed in hypoxic relative to normoxic cells at 72 hours (Figure 1F). Of

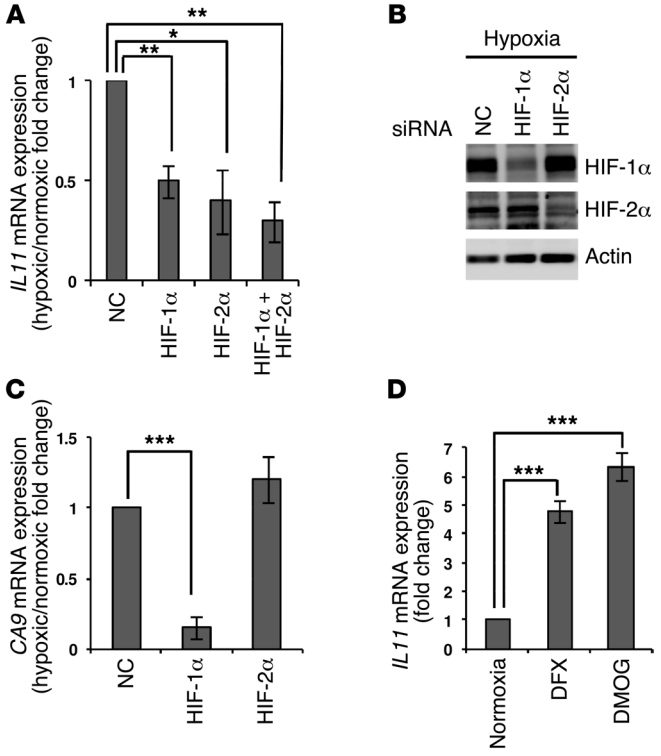

Figure 2
HIF-1α and HIF-2α are involved in the hypoxic induction of *IL11*. (**A**) PC3 cells were transfected with either NC siRNA or smartpool siRNA targeting HIF-1α and HIF-2α (25 nM). Twenty-four hours after transfection, cells were cultured under normoxia or hypoxia for an additional 24 hours. Results are presented as fold change of hypoxic induction of *IL11* mRNA expression, relative to normoxic PC3 cells transfected with NC siRNA, which is arbitrarily considered equal to 1 (mean ± SEM of 3 independent experiments; *t* test). (**B**) PC3 cells were transfected as described above and incubated under hypoxic conditions for an additional 24 hours. HIF-1α and HIF-2α protein levels were measured by Western blot analysis. (**C**) PC3 cells were cultured and transfected, and results are expressed as described in **A** (*t* test). (**D**) PC3 cells were treated with either DFX (100 μM) or DMOG (1 mM) for 24 hours under normoxic conditions, and *IL11* mRNA expression was assessed using quantitative RT-PCR. Results are expresses as mean ± SEM of 3 independent experiments (*t* test). $^{*}P < 0.05$, $^{**}P < 0.01$, $^{***}P < 0.001$.

note, *IL6* mRNA levels were not modulated by hypoxia in PC3 cells (data not shown), suggesting a differential sensitivity to oxygen deprivation of members of the IL-6 family of cytokines. These results demonstrate that *IL11* mRNA and IL-11 protein are induced by hypoxia in human cancer cell lines.

HIF-1α and HIF-2α contribute to hypoxic induction of IL11 mRNA in PC3 cells. To further investigate the role of HIFs in the induction of *IL11* mRNA expression, PC3 cells were transiently transfected with scrambled siRNA or siRNAs targeting HIF-1α or HIF-2α. Twenty-four hours following transfection, cells were incubated under hypoxic conditions for an additional 24 hours and levels of *IL11* and *CA9* mRNA were measured (Figure 2, A and C). siRNA silencing of the corresponding target was confirmed by Western blot analysis (Figure 2B). Hypoxic induction of *IL11* mRNA expression was decreased by 50% and 60% in cells transfected with HIF-1α and HIF-2α siRNA, respectively, relative to scrambled siRNA, suggesting that both HIF-1α and HIF-2α may play a role in the hypoxic induction of *IL11* mRNA expression in PC3 cells (Figure 2A). In contrast, hypoxic induction of *CA9* was decreased by more than 80% in cells transfected with HIF-1α, but not HIF-2α, siRNA (Figure 2C). Further evidence in support of the involvement of HIF in the hypoxic induction of *IL11* mRNA was provided by experiments conducted in the presence of desferrioxamine (DFX; 100 μM) or dimethyloxallyl glycine (DMOG; 1 mM), which block HIF degradation and promote normoxic accumulation of HIF (Figure 2D). Levels of *IL11* mRNA increased by 4.8- and 6.3-fold in cells treated with DFX or DMOG, respectively, relative to untreated cells (Figure 2D). Taken together, these results indicated that HIF is involved in the hypoxic induction of *IL11* expression, suggesting that other transcriptional pathways may contribute to induction of *IL11* mRNA expression in hypoxic cancer cells.

Von Hippel Lindau-dependent regulation of IL11 expression. Loss of function of the Von Hippel Lindau (*VHL*) tumor suppressor gene is associated with normoxic accumulation of HIF-1α and HIF-2α. We investigated the expression of *IL11* mRNA and protein in paired clear cell renal carcinoma cell lines either lacking a functional VHL (RCC4 and 786.O) or in which the VHL had been reintroduced (RCC4-VHL and WT2). RCC4 cells expressed high constitutive levels of *IL11* mRNA that were significantly decreased (approximately 90%) in RCC4-VHL cells (Figure 3A). A similar pattern of mRNA expression was observed for canonical HIF-regulated genes such as *CA9* and *VEGF* (Figure 3A). Similar results were observed in 786.O cells, which only express HIF-2α and in which much higher levels of *IL11*, *CA9*, and *VEGF* mRNA were detected relative to WT2 cells, in which VHL had been reintroduced (Figure 3B). In agreement with *IL11* mRNA expression, normoxic RCC4 cells secreted detectable levels of IL-11 protein (approximately 200 pg/ml), which were decreased by more than 50% in RCC4-VHL cells (Figure 3C). To investigate the relative contribution of HIF-1α and HIF-2α to *IL11* mRNA expression in VHL-deficient cells, RCC4 cells were infected with lentiviral particles expressing either a scrambled shRNA or shRNAs targeting HIF-1α or HIF-2α, respectively (Figure 3D). Consistent with previous reports, HIF-1α silencing selectively inhibited *CA9* mRNA expression, whereas HIF-2α silencing decreased expression of *VEGF* mRNA (Figure 3E). Interestingly, *IL11* mRNA expression was only marginally decreased by HIF-1α silencing, but was inhibited by more than 70% in cells silenced for HIF-2α relative to control cells expressing a scrambled shRNA (Figure 3E). These results demonstrate that *IL11* expression is regulated in a VHL-dependent manner and that HIF-2α is required for its expression in VHL-deficient cells, mirroring the regulation of *VEGF* mRNA.

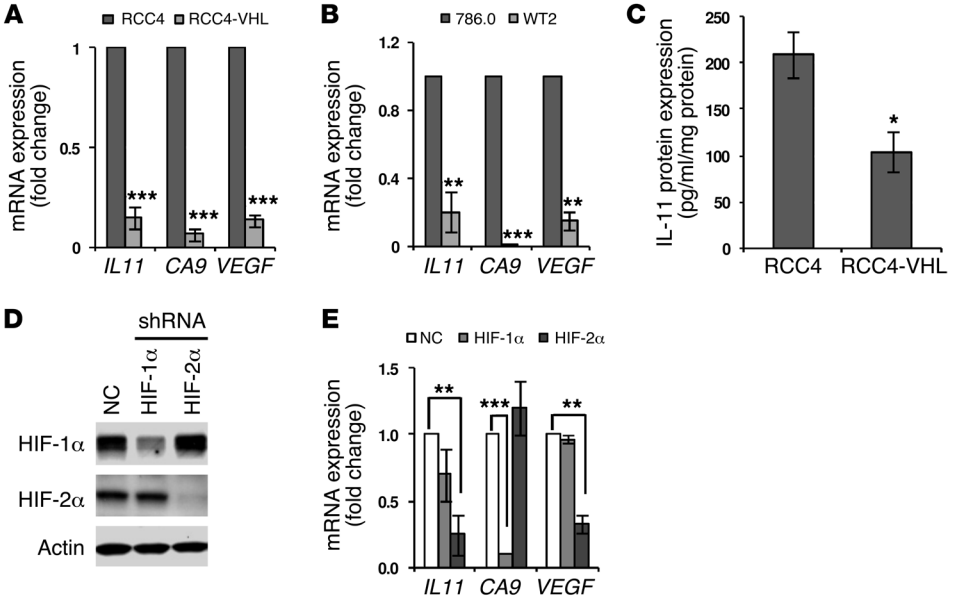

Figure 3

IL-11 expression is regulated in a VHL-dependent fashion. (**A**) RCC4 (VHL-deficient) and RCC4-VHL (VHL-reintroduced) cells were cultured under normoxic conditions for 24 hours. Quantitative RT-PCR results are expressed as fold change relative to mRNA levels detected in RCC4 cells (mean ± SEM of 3 separate experiments; *t* test). (**B**) WT2 (VHL-reintroduced) and 786.O cells were cultured under normoxic conditions as described above, and results are expressed as fold change relative to levels of mRNA detected in 786.O cells (mean ± SEM of 3 separate experiments; *t* test). (**C**) Levels of IL-11 protein were measured in supernatants harvested from RCC4 and RCC4-VHL cells cultured under normoxic conditions for 24 hours using a commercially available ELISA kit. Results are presented as fold increase relative to IL-11 protein levels detected in RCC4 cells, and were normalized for total protein content (mean ± SEM of 3 different experiments; *t* test). (**D**) Western blot analysis was used to assess levels of HIF-1α and HIF-2α protein in RCC4 NC, RCC4 HIF-1α KD, and RCC4 HIF-2α KD cells cultured under normoxic conditions. (**E**) RCC4 NC, RCC4 HIF-1α KD, and RCC4 HIF-2α KD cells were generated using lentiviral vectors expressing the corresponding shRNA. Levels of *IL11*, *CA9*, and *VEGF* mRNA expression were tested using quantitative RT-PCR in cells cultured under normoxic conditions. Results are expressed as fold change relative to RCC4 stably expressing a scrambled shRNA (NC) (mean ± SEM of 3 independent experiments; *t* test). $^*P < 0.05$; $^{**}P < 0.001$; $^{***}P < 0.0001$.

A cooperative interaction between HIF-1α and AP-1 mediates transcriptional activation of the IL11 promoter. To further investigate the transcriptional regulation of *IL11* expression by hypoxia, we cloned a 949-bp fragment (position –937 to +12) of the *IL11* gene in front of a promoter-less luciferase reporter plasmid. The 937-bp fragment contained a putative hypoxia response element (HRE) site at position –241 to –237 (5′-GCGTG-3′) and an AP-1 site at position –185 to –179 (5′-TGAGTCA-3′), the latter of which was previously implicated in transcriptional regulation of *IL11* expression (29). PC3 cells were transiently transfected with the full-length promoter or with plasmids in which the HRE and the AP-1 sites had been deleted or mutated, respectively, and they were then cultured under normoxic or hypoxic conditions for 24 hours before assessment of luciferase activity. Hypoxia failed to increase luciferase expression, relative to normoxia, in cells transfected with BO937 (position –937 to +12) or with BO272 (position –272 to +12), which contain both the HRE and AP-1 sites (Figure 4A). Surprisingly, further deletion from BO272 (plasmid BO223; position –223 to +12) of a 50-bp fragment encompassing the HRE site was associated with a 4.2-fold induction of luciferase expression in cells cultured under hypoxic conditions, relative to control cells. These results not only suggest the potential presence of sequences with repressor activity in the 50-bp deleted region, but they also indicate that the HRE was dispensable for the hypoxic induction of *IL11* promoter (Figure 4A). To address the functional role of the AP-1 site in the hypoxic induction of *IL11* transcriptional activity, we generated a construct in which the AP-1 site was mutated (BO185; CAT-GTCA, mutated sequence underlined). Notably, the vector with a mutated AP-1 site was no longer inducible by hypoxia, which demonstrated that the AP-1 site is indeed required for hypoxic inducibility of the *IL11* promoter (Figure 4A). Further support of this conclusion was provided by cotransfection experiments in which an AP-1 dominant-negative expression vector, which effectively inhibited AP-1 transcriptional activity (Supplemental Figure 2A), was able to completely abrogate hypoxic induction of BO223, containing the wild-type AP-1 site, in PC3 cells (Figure 4B). Overall, these results demonstrate that the AP-1 site, but not the HRE, is required for transcriptional activation of the *IL11* promoter by hypoxia in PC3 cells.

The above results (Figure 2A) indicated that HIF-1α was involved in the hypoxic induction of *IL11* mRNA expression in PC3 cells. We therefore tested whether HIF-1α was implicated in the hypoxic induction of *IL11* promoter activity. We found that hypoxic inducibility of plasmid BO223, which only contains the wild-type AP-1 site, was almost completely abrogated by cotransfection with siRNA targeting HIF-1α (Figure 4C), suggesting that despite the lack of a canonical HRE site in this promoter fragment,

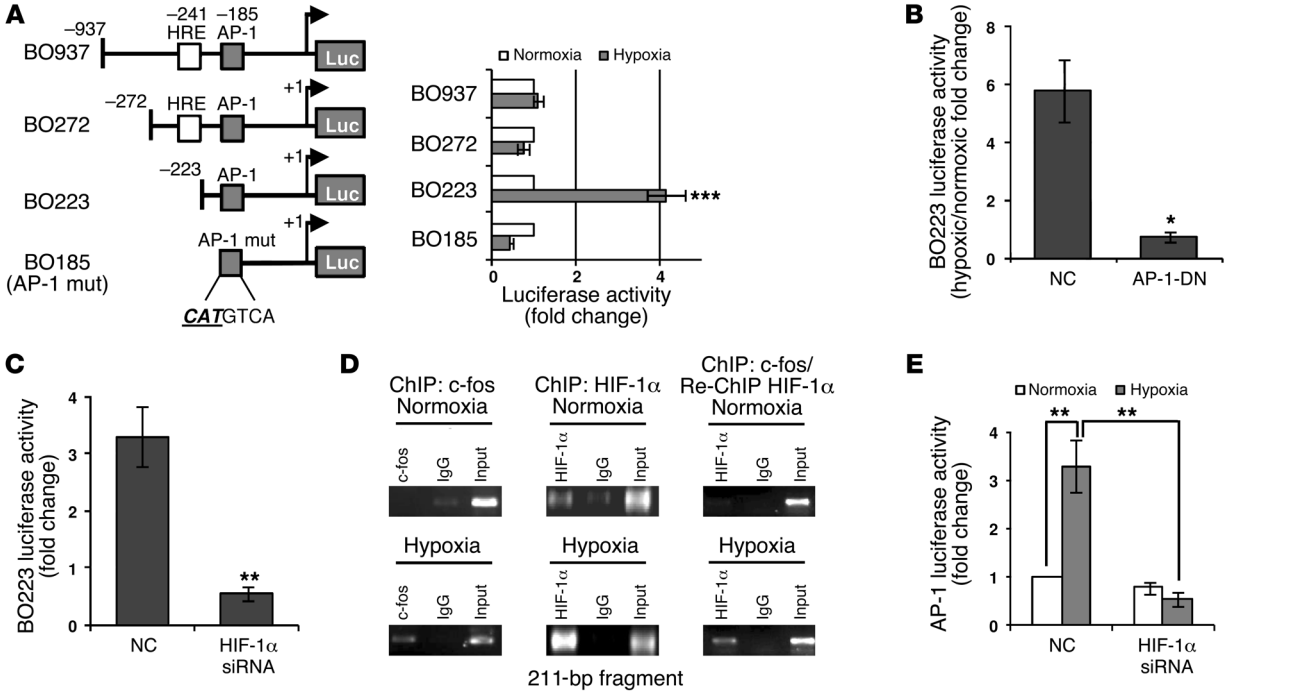

Figure 4

Cooperative interaction between AP-1 and HIF-1α mediates transcriptional activation of *IL11* promoter by hypoxia. (**A**) Left: Representation of *IL11* promoter constructs upstream of the luciferase gene. Right: PC3 cells were transfected with the indicated *IL11* promoter constructs. Twenty-four hours after transfection, cells were cultured under normoxia or hypoxia for an additional 24 hours before assessing luciferase activity. Results are expressed as a fold increase relative to the corresponding normoxic control (mean ± SEM of 3 independent experiments; *t* test). (**B**) PC3 cells were transfected with BO223 *IL11* promoter construct and cotransfected either with irrelevant plasmid DNA or with an AP-1 dominant-negative (DN) expression vector. Cells were cultured and harvested as described above. Results are expressed as hypoxic induction relative to normoxic PC3 cells (mean ± SEM of 3 separate experiments; *t* test). (**C**) PC3 cells were transfected with BO223 and cotransfected with either scramble siRNA or smartpool siRNA targeting HIF-1α. Cells were cultured and harvested as described above. (**D**) PC3 cells were cultured for 24 hours in normoxia or hypoxia, and ChIP assay was conducted as described in the Methods. Re-ChIP protocol was conducted on anti-fos samples using anti–HIF-1α antibody ($n = 2$). (**E**) PC3 cells were transfected with an AP-1 luciferase reporter plasmid and cotransfected with either scramble siRNA or smartpool siRNA targeting HIF-1α. Cells were cultured and harvested as described above (mean ± SEM of 3 separate experiments; *t* test). $^*P < 0.05$; $^{**}P < 0.001$; $^{***}P < 0.0001$.

HIF-1α does indeed contribute to the hypoxia inducibility of the *IL11* promoter. Further support for the involvement of HIF-1α in the hypoxic induction of BO223 was provided by cotransfection experiments with a constitutively active form of HIF-1α (HA-HIF1α P402A/P564A), which caused an increase in luciferase expression up to 13-fold in normoxia and 36-fold in hypoxia (Supplemental Figure 2B). A plasmid (pGL2TK-HRE) containing 3 copies of a canonical HRE upstream of the luciferase reporter gene was used as a control for the HIF-1–dependent inducibility of luciferase expression (Supplemental Figure 2C).

The HIF-1–dependent inducibility of BO223, an *IL11* promoter fragment that did not contain a canonical HRE sequence, led us to hypothesize that HIF-1 may be contributing to the hypoxic induction of AP-1 without being actively involved in DNA-binding activities. To address this question, ChIP experiments were performed in PC3 cells cultured under normoxic or hypoxic conditions for 24 hours, using anti-fos or anti–HIF-1α antibodies and primers amplifying the region that encompasses the AP-1 site (from position –369 to –172). As shown in Figure 4D, experiments using anti-fos antibodies confirmed that c-fos was bound to the AP-1 site in nuclear extracts of hypoxic, but not normoxic, PC3 cells. Surprisingly, a band of the appropriate size was also observed when experiments were performed with an anti–HIF-1α antibody, suggesting that HIF-1α may be recruited to the *IL11* promoter in the region containing the AP-1 site (Figure 4D). To further investigate whether HIF-1α was part of a transcriptional complex at the AP-1 site, we performed ChIP/re-ChIP experiments using first an anti-fos antibody and then an anti–HIF-1α antibody. Results from these experiments indicated that HIF-1α may indeed be part of a transcriptional complex at the AP-1 site, presumably in association with c-fos (Figure 4D). Amplification of a fragment containing an AP-1 site in the cyclin D1 promoter and amplification of a region containing the HRE sequence in the *VEGF* promoter region were used as positive controls for specific binding of c-fos and HIF-1α, respectively (Supplemental Figure 2D).

Finally, to further corroborate the interaction between HIF-1α and AP-1 in the hypoxic induction of transcriptional activity in PC3 cells, we demonstrated that induction of an AP-1 luciferase reporter plasmid by hypoxia was significantly decreased in the presence of siRNA targeting HIF-1α (Figure 4E). Overall, these results demonstrate that hypoxic transcriptional activation of *IL11* is mediated, at least in part, by a cooperative interaction between AP-1 and HIF-1α, which activate the *IL11* promoter.

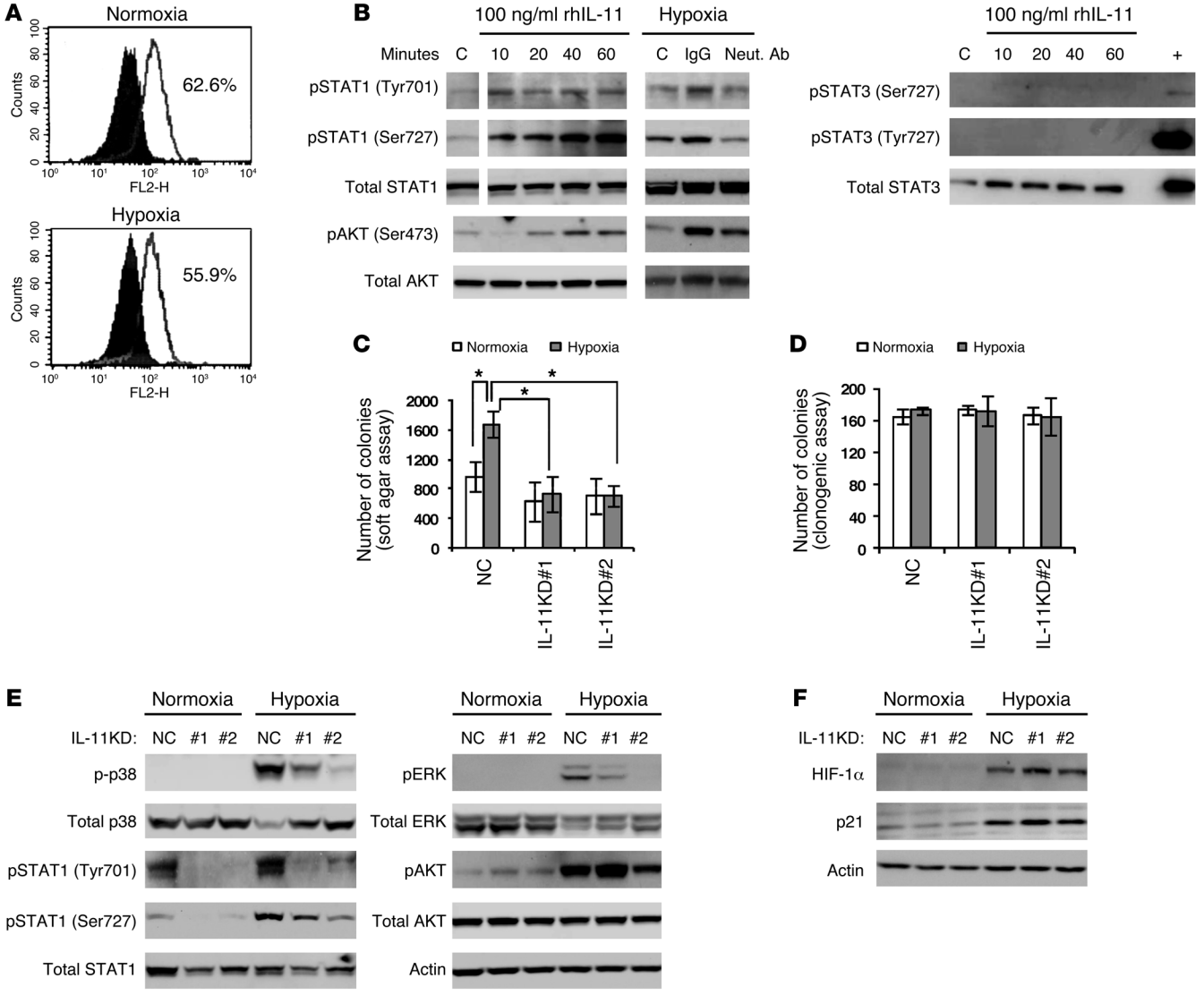

Figure 5

Autocrine induction of IL-11/IL-11Rα signaling in hypoxic PC3 cells. (**A**) PC3 cells were cultured under normoxic or hypoxic conditions for 24 hours and were tested for IL-11Rα expression by flow cytometric analysis as described in the Methods. (**B**) Left: PC3 cells were serum starved for 24 hours and then incubated in normoxia for the indicated times in the presence of 100 ng/ml of rhIL-11. Right: Serum-starved PC3 cells were cultured in normoxia or hypoxia for 48 hours in the absence or presence of a human IL-11–neutralizing antibody (50 ng/ml) or an isotype-matched control antibody (IgG). Levels of pSTAT1 (Tyr701 and Ser727), pAKT (Ser473), and pSTAT3 (Ser 727 and Tyr705) were assessed using Western blot. Results shown are representative of 2 independent experiments. C, untreated control; +, positive control. **(C)** PC3 NC, IL-11KD#1, and IL-11KD#2 cells were cultured under normoxic or hypoxic conditions for 24 hours and then plated in soft agar. Results shown are the average of 2 independent experiments (*t* test; $^*P < 0.05$). (**D**) PC3 NC, IL-11KD#1, and IL-11KD#2 cells were cultured under normoxic or hypoxic conditions for 24 hours and then plated. Colonies were stained after 10 days (mean ± SEM of 2 independent experiments). (**E**) PC3 NC, IL-11KD#1, and IL-11KD#2 cells were cultured as described for the right panel of **B**. Levels of total and phosphorylated ERK, AKT, p38, and STAT1 were measured using immunoblotting. (**F**) PC3 lysates were analyzed as described in **E**. Results are representative of 3 experiments.

Hypoxic induction of IL-11 triggers autocrine activation of signaling pathways in PC3 cells. The functional role of IL-11 in human cancer is poorly understood. We hypothesized that hypoxic induction of IL-11 may act in an autocrine fashion in PC3 cells. To address this possibility, we used flow cytometric analysis to investigate the expression and regulation of IL-11Rα, the specific subunit that mediates IL-11 signaling, in PC3 cells. As shown in Figure 5A, IL-11Rα was constitutively expressed in approximately 60% of PC3 cells, and its levels were not significantly changed under hypoxic conditions. We next investigated whether the presence of IL-11Rα in PC3 cells was associated with activation of downstream signaling pathways. As shown in Figure 5B, addition of recombinant human IL-11 (rhIL-11; 100 ng/ml) to PC3 cells under normoxic conditions was sufficient to trigger rapid phosphorylation of STAT1 (Tyr701 and Ser727) and AKT (Ser473); however, under these experimental conditions we were unable to detect either tyrosine or serine phosphorylation of STAT3. More importantly, the addition of

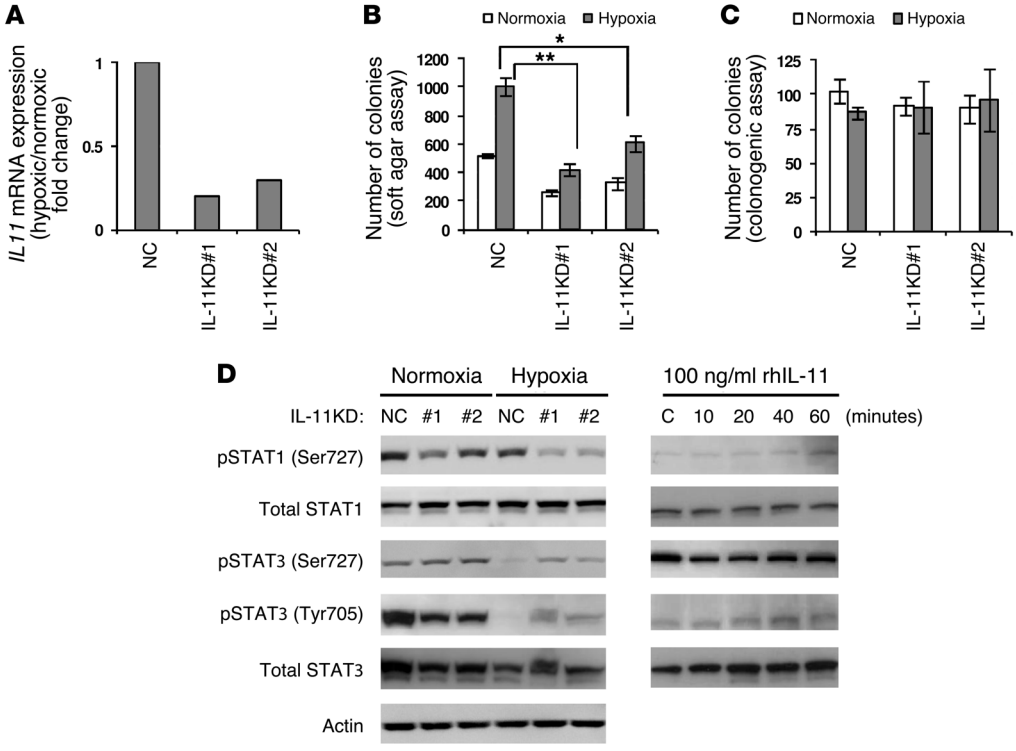

Figure 6

Phenotype and signaling effects in IL-11 knockdown HCT116 cells. (**A**) HCT116 NC, IL-11KD#1, and IL-11KD#2 cells were generated using lentiviral vectors expressing the corresponding shRNA. Levels of *IL11* mRNA expression were tested using quantitative RT-PCR in cells cultured under normoxic or hypoxic conditions for 24 hours. Results are expressed as fold increase relative to normoxic HCT116 NC cells. (**B**) HCT116 NC, IL-11KD#1, and IL-11KD#2 cells were cultured under normoxic or hypoxic conditions for 24 hours and then plated in soft agar. The graph reports the number of colonies detected after 13 days of growth in soft agar. Results shown are the average of 2 independent experiments (*t* test; $^{*}P < 0.05$, $^{**}P < 0.001$). (**C**) HCT116 NC, IL-11KD#1, and IL-11KD#2 cells were cultured under normoxic or hypoxic conditions for 24 hours and then plated. Colonies were stained after 10 days (mean ± SEM of 2 independent experiments). (**D**) Left: HCT116 NC, IL-11KD#1, and IL-11KD#2 cells were serum starved for 24 hours and cultured for an additional 48 hours under normoxic or hypoxic conditions. Levels of phosphorylated STAT1 (Ser727) and STAT3 (Ser 727 and Tyr705) were assessed using Western blot. Actin was assessed as an internal control. Right: HCT116 cells were serum starved for 24 hours and then incubated in normoxia for the indicated times in the presence of 100 ng/ml of rhIL-11. Levels of pSTAT1 (Ser727) and pSTAT3 (Ser 727 and Tyr705) were assessed using Western blot. Results shown are representative of 2 independent experiments.

an IL-11–neutralizing antibody was able to almost completely abrogate hypoxic induction of pSTAT1 (Tyr701 and Ser727) and pAKT, further demonstrating that: (a) PC3 cells express a functional IL-11Rα; and (b) hypoxic induction of IL-11 triggers downstream signaling pathways in an autocrine fashion.

To further investigate the functional role of IL-11, we generated PC3 cells in which IL-11 expression was silenced using lentiviral vectors expressing 2 distinct shRNA sequences targeting IL-11 (IL-11KD#1 and IL-11KD#2), as well as control shRNA targeting luciferase (negative control [NC]). Hypoxic induction of *IL11* mRNA and IL-11 protein was decreased by more than 90% in IL-11KD#1 and IL-11KD#2 relative to NC cells (Supplemental Figure 3, A and B), confirming that these cells are silenced for IL-11 expression. We then investigated whether IL-11 was involved in the hypoxic induction of anchorage-independent growth. PC3 cells were incubated under normoxic or hypoxic conditions for 24 hours and tested for anchorage-independent growth and clonogenic survival on plastic. Cells cultured under hypoxic conditions were more clonogenic in soft agar, but not on plastic, relative to normoxic cells (Figure 5, C and D). Notably, the clonogenic advantage conferred by hypoxia was completely abrogated in cells silenced for IL-11, strongly suggesting that IL-11 may contribute to the increased tumorigenicity observed in hypoxic cells. On the contrary, IL-11 silencing had no significant effect on clonogenic survival on plastic, either under normoxic or hypoxic conditions (Figure 5D), ruling out the possibility that an effect on survival would be sufficient to account for the increased clonogenicity observed in anchorage-independent growth. More importantly, no significant differences in proliferative capacity (Supplemental Figure 3C), apoptosis (Supplemental Figure 3D), or cell cycle (Supplemental Figure 3E) were observed between control cells and cells silenced for IL-11, cultured either under normoxic or hypoxic conditions.

Results shown thus far clearly indicate that hypoxic PC3 cells express both IL-11 and IL-11Rα and that IL-11 may act in an autocrine fashion to mediate increased clonogenic potential of hypoxic cells. To further dissect the signal transduction pathways triggered by IL-11 in hypoxic cells, we investigated activation of relevant signaling molecules in PC3 NC cells and IL-11–silenced cells cultured under normoxic or hypoxic conditions for 48 hours. Relative to normoxia, incubation under hypoxia triggered phosphorylation of ERK1/2, AKT, p38, and STAT1 (Tyr701 and Ser727) in NC cells

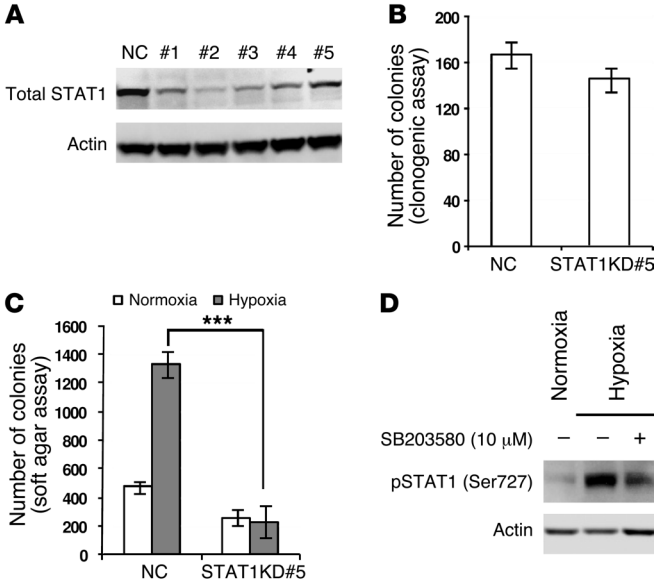

Figure 7
STAT1 and p38 mediate IL-11–dependent responses under hypoxia. (**A**) PC3-stable STAT1 knockdown cells were generated using lentiviral vectors expressing the corresponding shRNA. Total protein lysates were prepared and analyzed using Western blot analysis as described in the Methods. Actin was assessed as an internal control. (**B**) PC3 NC and STAT1KD#5 cells were cultured under normoxic conditions for 24 hours and then plated. Colonies were stained after 10 days (mean ± SEM of 3 independent experiments). (**C**) PC3 NC and STAT1KD#5 cells were cultured under normoxic or hypoxic conditions for 24 hours and then plated in soft agar. Results shown are the average of 2 independent experiments (*t* test; ***$P < 0.0001$). (**D**) PC3 cells were serum starved for 24 hours and treated with SB203580 (10 μM), a known p38 inhibitor, for an additional 48 hours under normoxia or hypoxia. Protein lysates were prepared and analyzed using Western blot analysis as described in the Methods. Actin was assessed as an internal control. Results shown are a representative experiment of 3 independent experiments.

(Figure 5E). The activation of p38, pSTAT1, and MAPK was significantly impaired in IL-11–silenced PC3 cells, although to a slightly different extent in IL-11KD#1 and IL-11KD#2, further emphasizing the existence of an autocrine signaling loop mediated by IL-11 under hypoxic conditions. On the contrary, IL-11 silencing did not impair hypoxic induction of HIF-1α and p21 (Figure 5F), demonstrating selective inhibition of hypoxic signaling pathways. In conclusion, these results demonstrate that autocrine production of IL-11 activates relevant signaling pathways that may contribute to the tumorigenic potential of hypoxic cancer cells.

Hypoxic induction of IL-11 mediates activation of signaling pathways in HCT116 and RCC4 cells. To address whether hypoxic induction of IL-11–dependent signaling pathways may play a role in other tumor types, we generated HCT116 colon cancer cells IL-11 knockdown (IL-11KD#1 and IL-11KD#2). *IL11* mRNA was decreased by more than 70% in IL-11KD#1 and IL-11KD#2 relative to NC cells (Figure 6A). Interestingly, IL-11 knockdown almost completely abrogated the hypoxic induction of anchorage-independent growth in HCT116 cells, but did not significantly affect clonogenic survival on plastic (Figure 6, B and C), consistent with what was observed in PC3 cells. To further dissect the signaling pathways activated by IL-11 in HCT116, we cultured cells in the presence of rhIL-11 under normoxic conditions. As shown in Figure 6D, rhIL-11 (100 ng/ml) induced a 3-fold increase in phosphorylation of STAT1 (Ser727) and a 2-fold increase in pSTAT3 (Tyr705). Notably, pSTAT3 Ser727 was constitutively present and did not change with addition of IL-11, while pSTAT1 Tyr701 was not detectable under these experimental conditions. More importantly, levels of pSTAT1 were significantly decreased in IL-11KD#1 and IL-11KD#2 cultured under hypoxic conditions; in contrast, pSTAT3 (Tyr705) was decreased under normoxic conditions in IL-11 knockdown cells, but slightly increased under hypoxia (Figure 6D). It is important to point out that STAT3 phosphorylation was significantly reduced under hypoxic conditions, relative to normoxic conditions, while STAT1 phosphorylation remained unchanged, possibly indicating a differential role of these proteins under normoxic and hypoxic conditions in HCT116 cells. Similar results, in terms of modulation of STAT1 and STAT3 signaling pathways by rhIL-11 and IL-11 knockdown, were observed in RCC4 renal cancer cells (Supplemental Figure 4), suggesting that hypoxic induction of IL-11 is functionally relevant in multiple human cancer cells. In conclusion, these results further support the conclusion that autocrine production of IL-11 activates relevant signaling pathways that may contribute to the tumorigenic potential of hypoxic cancer cells.

STAT1 mediates the IL-11–dependent tumorigenic phenotype of hypoxic cells. To further characterize the signaling pathways that mediate IL-11–dependent clonogenic phenotype in hypoxia, we silenced STAT1 in PC3 cells using lentiviral vectors expressing 5 distinct shRNA sequences (STAT1KD#1-5), as well as control shRNA targeting luciferase (NC) (Figure 7A). As shown in Figure 5E, IL-11 knockdown only partially inhibited STAT1 phosphorylation; thus, we used STAT1KD#5 cells, in which partial downregulation of STAT1 was observed, to further assess the role of STAT1 in IL-11–dependent responses. Consistent with proliferation studies in IL-11 knockdown cells, inhibition of STAT1 by 40% (STAT1KD#5) did not significantly affect PC3 clonogenic survival on plastic (Figure 7B), while almost complete STAT1 knockdown (STAT1KD#1–4) did affected clonogenic survival on plastic (50%–90% decrease; data not shown). Notably, even partial downregulation of STAT1 in PC3 cells (STAT1KD#5) completely abrogated hypoxia-dependent clonogenic survival advantage in soft agar (Figure 7C). These results are consistent with what was observed in IL-11 knockdown cells (Figure 5C), and they strongly suggest that STAT1 is involved in the IL-11–dependent tumorigenic phenotype induced in PC3 cells under hypoxic conditions.

STAT1 activation under hypoxia, in particular phosphorylation at Ser727, has been previously attributed to p38 activation. As shown in Figure 5E, p38 phopshorylation was indeed induced under protracted hypoxia, a phenomenon that was almost completely abrogated by IL-11 knockdown. To evaluate the role that p38 plays in STAT1 activation under hypoxia, PC3 cells were treated with SB203580, a known p38 inhibitor. As shown in Figure 7D, inhibition of p38 significantly decreased hypoxia-induced STAT1 Ser727 phosphorylation, providing evidence that IL-11–dependent STAT1 phosphorylation may indeed be mediated by p38.

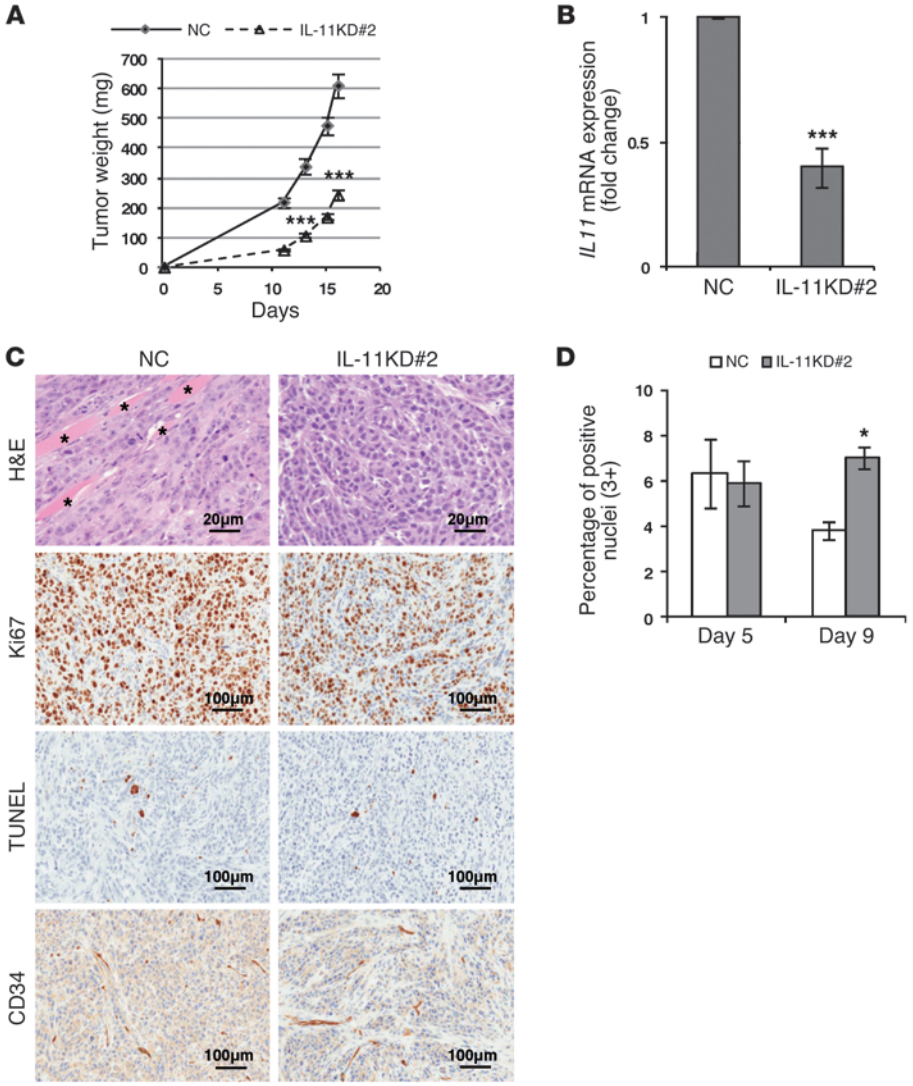

Figure 8
IL-11 knockdown impairs the growth of PC3 xenografts. (**A**) PC3 NC and IL-11KD#2 cells were injected s.c. into nude mice (26 mice/group), and tumor weight was measured as described in the Methods. Tumor incidence was 100% for both cell lines. A statistically significant difference was observed for tumor weight in mice injected with IL-11KD#2 compared with PC3 NC cells (*t* test; ***$P < 0.0001$). (**B**) *IL11* mRNA levels in IL-11KD#2 tumor lysates were measured using quantitative RT-PCR in tumor tissue harvested on day 16. Results are presented as mean ± SEM (10 mice/group). ***$P < 0.001$ versus PC3 NC tumors. (**C**) H&E (original magnification, ×40; scale bars: 20 μm) and Ki67, TUNEL, and CD34 staining (original magnification, ×20; scale bars: 100 μm) of representative tumor sections from PC3 NC and IL-11KD#2 tumors harvested on day 16. Asterisks indicate muscle fibers. (**D**) Percentage of TUNEL-positive nuclei (3^+, positive nuclei with intensity score 3 being the highest) in PC3 NC and IL-11KD#2 tumors at day 5 and day 9. (*t* test; *$P < 0.01$).

Taken together these results demonstrate that induction of IL-11 under hypoxic conditions triggers p38 and STAT1 activation and that STAT1 may be an important component of the oncogenic signaling pathways activated by IL-11 under hypoxia.

IL-11 knockdown impairs tumor growth in xenograft models. To validate the potential role of IL-11 in mediating tumor progression in in vivo models, PC3 NC, IL-11KD#1, and IL-11KD#2 cells were injected s.c. into female nude mice ($n = 26$/group) and tumor growth was monitored. Tumors from PC3 NC cells reached approximately 220 mg at day 11 and 613 mg at day 16 following injection. IL-11 knockdown resulted in significantly smaller tumors both on day 11 (26.5% and 48.4% for IL-11KD#2 and IL-11KD#1 cells, respectively, relative to PC3 NC cells) and on day 16 (39.6% and 73.3% for IL-11KD#2 and IL-11KD#1 cells, respectively, relative to PC3 NC cells) (Figure 8A and Supplemental Figure 5A). However, after an initial growth delay, tumors from IL-11–silenced cells seemed to regain a growth rate similar to PC3 control cells despite the fact that we confirmed that IL-11 knockdown was maintained in tumors originated from IL-11KD#2 (Figure 8B) and IL-11KD#1 cells (Supplemental Figure 5B) relative to PC3 NC cells.

To gain more insight into the potential mechanism(s) by which growth of IL-11 knockdown cells was impaired in vivo, we analyzed tumor tissues from PC3 NC and IL-11KD#2 cells harvested at day 16 for morphology (H&E), proliferation (Ki67), apoptosis (TUNEL), and microvessel density (CD34) (Figure 8C). PC3 NC tumors showed more necrosis and muscle invasion relative to tumors originating from IL-11–silenced cells, which remained encapsulated and showed little or no necrosis. Although these features might, at least in part, be accounted for by a difference in size, they may also be related to the less aggressive phenotype of IL-11 knockdown tumors. However, levels of Ki67 (proliferation), number of TUNEL-positive cells (apoptosis), and microvessel density (CD34-positive cells) were not significantly different between PC3 NC and IL-11KD tumors (Figure 8C). Moreover, no significant changes in phosphorylation of STAT1, AKT, mTOR, and p38 were detected between control and IL-11–silenced tumors harvested on day 16 (data not shown). These results led us to hypothesize that the defining difference between the PC3 NC and IL-11KD#2 tumors had to occur at an earlier stage of tumorigenesis, consistent with the hypoxia inducibility of IL-11 and the notion that approximately 50%–60% of PC3 cells express the

IL-11Rα. To address this question, an additional in vivo experiment was conducted in which tumors were harvested and morphology examined at day 5 and day 9 from implantation. Indeed, IL-11KD#2 tumors harvested on day 9 showed a significantly higher percentage of apoptotic nuclei relative to PC3 NC tumors (Figure 8D). In conclusion, our data demonstrate that inhibition of IL-11 expression impairs in vivo growth of prostate cancer cells, and our findings are consistent with an effect of IL-11 at an early stage of tumorigenesis.

Discussion

The identification of signaling pathways required for survival of hypoxic cancer cells may provide new opportunities for therapeutic intervention. The aim of this study was to identify functionally relevant pathways activated by chronically hypoxic cancer cells. We discovered that *IL11* is a novel hypoxia-inducible and VHL-regulated gene in human cancer cells. The expression of IL-11 and its receptor (IL-11Rα) has been extensively described in several human malignancies, including but not limited to prostate cancer and osteosarcoma (30–39), suggesting its potential involvement in human tumorigenesis. However, the regulation of IL-11 expression is still poorly understood and its contribution, if any, to tumor progression is not known. We provide evidence that IL-11 triggers activation of autocrine signaling pathways that may contribute to the tumorigenic phenotype of hypoxic stressed cancer cells and ultimately to tumor progression.

IL11 is an oxygen- and VHL-regulated gene. IL-11 is a member of the IL-6 family of cytokines, which signals through a common gp130 component and a specific IL-11Rα subunit (14). IL-11 is produced by a number of mesenchymal cells (40) and more recently its expression has been reported in several types of cancers, where it has been found to correlate with a more aggressive phenotype (23–28, 31–34, 38, 41–43). However, the functional role, if any, of IL-11 in human cancers is poorly understood. We found that *IL11* mRNA (and IL-11 protein) is induced in a number of human cancer cell lines incubated under hypoxic conditions for 24–72 hours. Moreover, our data indicate that HIF-1 is involved in the regulation of IL-11 expression. This conclusion is supported by (a) experiments using siRNA silencing HIF-1α or HIF-2α, which showed that both subunits may contribute to its regulation in solid tumors; (b) VHL-dependent regulation of IL-11, in VHL-deficient cells, IL-11 expression mirrored that of canonical VHL-regulated genes, such as *VEGF* and *CA9* (44), and was dependent on HIF-2α, consistent with the predominant role of HIF-2α in clear cell renal cell tumorigenesis (45); (c) normoxic induction of IL-11 in cells treated with DFX or DMOG, which block HIF-1 degradation. Thus, *IL11* can be added to the growing list of HIF-regulated genes. Interestingly, it has been recently shown that IL-11 increases HIF-1α nuclear translocation and transcriptional activity in human renal proximal tube cells during ischemia reperfusion, suggesting the existence of a positive feedback loop between IL-11 and HIF-1 (46).

Experiments conducted using a 949-bp fragment of the *IL11* promoter further demonstrated a complex mechanism of regulation involving AP-1 in cooperation with HIF-1α. AP-1 has been previously implicated in IL-11 transcriptional activation by other signals (29, 47, 48). We demonstrated that AP-1 is indeed important to activate the *IL11* promoter under hypoxic conditions using 2 different approaches: mutation of the AP-1 binding site and expression of an AP-1 dominant-negative protein. Moreover, our results indicated that HIF-1α appeared to be part of a transcriptional complex at the AP-1 site, yet without direct DNA binding activity. Accordingly, the hypoxic induction of the *IL11* promoter fragment containing the AP-1 site was abrogated by HIF-1α silencing, thus providing evidence that HIF-1α plays a crucial role for hypoxic activation of AP-1. These findings are consistent with previous reports indicating that HIF-1 may be involved in activation of AP-1 by chronic hypoxia, by either inducing c-Jun or by increasing its phosphorylation (49–51). Indeed, hypoxia did increase c-Jun phosphorylation under our experimental conditions (Supplemental Figure 6A). Notably, inhibition of c-Jun phosphorylation using the JNK inhibitor SP600125 decreased *IL11* mRNA accumulation under hypoxia, but not VEGF expression, and did not affect HIF-1α accumulation (Supplemental Figure 6, C and D), suggesting that IL-11 upregulation by hypoxia is dependent on c-Jun. Notably, hypoxia induces c-fos binding to the AP-1 site in the *VEGF* promoter, yet HIF-1α does not interact with c-fos on the *VEGF* promoter, suggesting that the cooperative regulation of IL-11 by AP-1 and HIF-1 is not a general phenomenon (Supplemental Figure 6B). In addition, HIF-1 may exert transcriptional regulatory functions without DNA binding activity, for instance in the regulation of p21 expression by counteracting c-MYC activity (52), consistent with the regulatory role of HIF-1 proposed in our model.

Activation of autocrine signaling pathways by IL-11. A major finding of our study was that, concomitant with hypoxic induction of IL-11; human cancer cells expressed a functional IL-11Rα subunit, which is required for IL-11 signaling. Although IL-11Rα expression has been previously reported in cancer cells, its functional role, if any, in tumorigenesis remains to be determined (34). We demonstrated that hypoxic induction of IL-11 triggers autocrine signaling pathways in cancer cells, which may contribute to the increased tumorigenicity conferred by hypoxia to chronically stressed cells. The existence of an autocrine pathway induced by IL-11 was clearly shown by experiments using an IL-11–neutralizing antibody, which was able to completely block hypoxic induction of STAT1 phosphorylation and by shRNA-mediated silencing of IL-11, which blocked hypoxic induction of pERK, p38, and pSTAT1 (Tyr701 and Ser727) in PC3 cells. In contrast, IL-11 silencing did not affect expression of HIF-1α or p21, suggesting a coherent signaling pattern associated with the gp130/IL-11Rα receptor signaling complex. Similar effects on autocrine activation of IL-11–dependent signaling pathways were observed in at least 2 other cell lines in which IL-11 had been silenced, demonstrating that this phenomenon is not restricted to prostate cancer cells.

Our in vitro studies on cells silenced for IL-11 did not show any relevant phenotype relative to wild-type cells, at least in terms of proliferation, cell cycle, induction of apoptosis, or clonogenic survival on plastic. In contrast, a dramatic decrease in anchorage independent growth was consistently seen. In an attempt to elucidate the molecular mechanism underlying IL-11–mediated anchorage independent growth, we examined several pathways that are elicited by the gp130 family of cytokines. It is notable that we were unable to detect STAT3 phosphorylation in PC3 cells, despite detectable levels of STAT3 protein. Indeed, conflicting findings regarding STAT3 phosphorylation and locus deletion in PC3 cells have been reported in the literature (53–57). Nevertheless, total and partial STAT3 knockdown significantly decreased PC3 cell proliferation, a finding inconsistent with the phenotype of IL-11 knockdown cells, yet suggesting that STAT3 does play an impor-

tant oncogenic role in PC3 cells (data not shown). In contrast, rhIL-11 did increase STAT3 phosphorylation in HCT116 and RCC4 cells, indicating that distinct transcriptional elements may be activated by IL-11 in different cancer cell lines and that STAT3 does play a role in IL-11–dependent signaling pathways. Conversely, we were able to show STAT1 phosphorylation, not only at Tyr701, which is presumably associated with JAK signaling, but also at Ser727, which under our experimental conditions appeared to be dependent upon p38 phosphorylation (Figure 6). Activation of STAT1 by p38 has been previously reported (58). Although the role of STAT1 in tumorigenesis is still controversial (59), we show that partial STAT1 knockdown completely inhibited hypoxia-induced, anchorage-independent cell growth in a similar fashion to what was observed in IL-11 knockdown in PC3 cells, strongly suggesting that STAT1 is involved in mediating the tumorigenic phenotype triggered by IL-11 under hypoxic conditions. In contrast, partial STAT1 knockdown did not significantly affect PC3 proliferation, consistent with the effects observed in IL-11 knockdown cells. Interestingly, STAT3 phosphorylation, but not STAT1 phosphorylation, was significantly decreased in HCT116 cells cultured under hypoxic relative to normoxic conditions, suggesting that STAT1 and STAT3 may play distinct roles under normoxic and hypoxic conditions. Overall, these data suggest that STAT1 may be an important component in signaling pathways triggered by a hypoxia-stressed tumor microenvironment.

Potential mechanism of impaired tumor growth in vivo. The most exciting finding of our study is that growth of IL-11–silenced cells in nude mice was significantly decreased compared with PC3 NC cells, a result consistently observed in 2 independent experiments using 2 distinct shRNA sequences targeting IL-11. These data clearly indicate that IL-11 contributes to tumor growth in vivo, at least in part dependent upon its induction by intratumoral hypoxia. Consistent with this conclusion, IL-11 knockdown cells showed an increase in apoptotic cell death at early but not late stages of tumorigenesis, suggesting that IL-11 may play a prosurvival role at a time when incipient hypoxia is induced in the tumor microenvironment. The profound inhibition of signaling pathways observed in IL-11–silenced cells, which included a decrease of MAPK, p38, and STAT1 phosphorylation, is consistent with gp130-mediated signaling events, and provides a rational mechanism for the delayed tumor growth observed in xenograft experiments. It is conceivable that inhibition of a complex network of gp130-dependent signaling pathways in IL-11–silenced cells may be responsible for the impaired tumor growth observed. Accordingly, cancer cells expressing the IL-11Rα subunit (approximately 50% in PC3 cells) may have a survival disadvantage at a time when increased production of IL-11, triggered by intratumoral hypoxia, may mediate its effects on IL-11Rα–expressing cells. The latter explanation is consistent with the pattern of delayed growth observed in IL-11–silenced tumors, which eventually appeared to regain the growth rate of wild-type cells. Finally, the possibility that IL-11 may also contribute to tumor progression by paracrine effects on the tumor microenvironment, including but not limited to angiogenesis and immune regulation, will have to be further analyzed. Notably, IL-11–silenced tumors did not show differences in microvessel density relative to control tumors, both at early and late stages of tumor progression (data not shown and Figure 7C), suggesting that angiogenesis may not be an important pathway mediated by IL-11 in our experimental model.

IL-11, a novel therapeutic target for hypoxic cancer cells. While IL-6 has been implicated as a tumor-promoting factor in several human malignancies, the potential role of IL-11 in human tumorigenesis has been largely neglected. However, over the last few years, evidence has been provided implicating IL-11 in models of inflammation and cancer and associating its expression with a metastatic phenotype and poor prognosis (20–25, 27, 36, 41). Our data identify the IL-11/IL-11Rα axis as a pathway utilized by hypoxia-"stressed" cancer cells and as a potential target for therapy. The IL-11/IL-11Rα pathway is amenable to therapeutic intervention, by targeting either the specific receptor or the ligand. Indeed, the recent success in the development of effective therapeutic treatments using monoclonal antibodies targeting growth factors and their receptors provide further support for this approach. Finally, the possibility that the IL-11/IL-11Rα pathway be relevant for the growth of VHL-deficient cells remains to be further investigated in order to fully appreciate the potential therapeutic applications of this strategy.

Methods

Cell lines and reagents. Human cancer cell lines PC3, MCF7, HCT116, IGROV1, NCI-H460, UACC-62, KM12, 786.0, and OVCAR-5 were obtained from the NCI-60 Human Tumor Cell Line Screen (Frederick National Laboratory for Cancer Research) and maintained in RPMI-1640 supplemented with L-glutamine, 50 IU/ml penicillin, 50 μg/ml streptomycin, and 5% FBS (Hyclone). Renal RCC4, RCC4-VHL, and WT2 cells were grown in DMEM supplemented with 10% FBS. Cells were normally grown at 37°C in 5% CO_2 and ambient oxygen (normoxic conditions). Hypoxia was achieved in an Invivo$_2$ 400 hypoxic workstation (Ruskinn Technologies) set to deliver 1% oxygen in 5% CO_2 at 37°C. PMA, DFX, and SP600125 were from Sigma-Aldrich. DMOG was purchased from Cayman Chemicals. rhIL-11– and IL-11–neutralizing antibody were purchased from R&D Systems.

Generation of target-specific silenced cells. Lentiviral particles were produced in 293FT cells by transient transfection of pLKO.1 plasmids harboring specific shRNA targeting luciferase, IL-11, HIF-1α, HIF-2α, or STAT1 (Open Biosystems) with packaging vectors. Transfection was performed with FuGene6 (Roche Applied Science) according to the manufacturer's instructions. After 24 hours, transfection complexes were removed and cells were incubated with fresh complete DMEM (10% FBS) for an additional 24 hours. Supernatant was then collected and filtered using 0.45-μm filters. Viral titers were determined using the Lenti-X qRT-PCR Titration Kit (Clontech Laboratories Inc.) according to the manufacturer's instructions. Target cells (RCC4 or PC3) were incubated with the viral supernatant at a multiplicity of infection of 5 in the presence of 8 μg/ml polybrene (Sigma-Aldrich). Twenty-four hours after infection, cells were selected with puromycin (2 μg/ml) for 3 days.

Reporter plasmids. Different fragments of the human *IL11* promoter were amplified from the S121676 pSGG_prom plasmid (SwitchGear Genomics) containing the region (–975 bp; +80 bp) of the *IL11* gene, using the primers listed in Table 1. PCR amplifications were performed using primers incorporating restriction sites for MluI (forward primer) and BglII (reverse primer), which allowed for insertion of the amplicons in the multiple cloning site of the linearized pSGG_prom plasmid, upstream of the luciferase gene. The vector pGL2-TK-HRE was used as an internal control for hypoxic induction of HIF-1α transcriptional activity and has been previously described (60). The AP-1 luciferase reporter plasmid and the AP-1 dominant-negative expression vector were a gift from Nancy Colburn at the National Cancer Institute (Frederick, Maryland, USA).

Table 1
Primers used to generate *IL11* promoter plasmids

Plasmid	Promoter region	Primer	Sequence[A]
BO937	Position –937 to +12	Forward	5′-TGAT*ACGCGT***CCAACATCTCAGCGTCTCTGTCTT**-3′
		Reverse	5′-ACTG*AGATCT***TTTAACCCTTCCCTGTCCGCT**-3′
BO272	Position –272 to +12	Forward	5′-TGAT*ACGCGT***TTTCCTTCCGTGCCCTCCT**-3′
		Reverse	5′-ACTG*AGATCT***TTTAACCCTTCCCTGTCCGCT**-3′
BO223	Position –223 to +12	Forward	5′-TGAT*ACGCGT***AGCCGCTCCGTCTGAATGGAAA**-3′
		Reverse	5′-ACTG*AGATCT***TTTAACCCTTCCCTGTCCGCT**-3′
BO185	Position –185 to +12	Forward	5′-TGAT*ACGCGT***CATGTCAGGATGTGTCAGGCCG**-3′
		Reverse	5′-ACTG*AGATCT***TTTAACCCTTCCCTGTCCGCT**-3′

[A]Tail + restriction site (underlined italic) + specific sequence (bold).

Transient transfection and luciferase activity. PC3 cells were seeded in 48-well plates (15,000 cells per well) and transiently transfected with luciferase reporter plasmids containing different fragments of the *IL11* promoter either with an irrelevant DNA plasmid or with a vector expressing a stable form of HIF-1α (HA-HIF1α P402A/P564A-pBabe-puro, plasmid 19005; Addgene) (61), using FuGene6 (Roche Applied Science) according to the manufacturer's instructions. Twenty-four hours following transfection, cells were cultured under normoxic or hypoxic conditions for an additional 24 hours and luciferase levels were measured using the Luciferase Assay System with Reporter Lysis Buffer kit (Promega). Luciferase levels were normalized to protein content for each condition.

siRNA transfection. Specific smartpool siRNAs for HIF-1α, HIF-2α, and NC siRNA were transfected using oligofectamine (Invitrogen) according to the manufacturer's instructions. Briefly, siRNA complexes were added to subconfluent cells and then incubated in serum-free condition for 5 hours at 37°C. The medium was then changed to RPMI with 5% FBS, and cells were incubated for an additional 24 hours before treatment, as indicated in the figures. NC siRNA was the "All Star Negative" control siRNA (QIAGEN); siRNAs targeting HIF-1α, HIF-2α, and IL-1α were siGENOME SMARTpool siRNAs (Darmacon).

Cotransfection of plasmid DNA with siRNA. PC3 cells were seeded in 48-well plates (15,000 cells per well) and transiently transfected with 125 ng plasmid DNA alone or with 10 nM siGENOME SMARTpool siRNAs, using Effectene Transfection Reagents (QIAGEN) according to the manufacturer's instructions. Twenty-four hours following transfection, cells were cultured under normoxic or hypoxic conditions for an additional 24 hours, and luciferase levels were measured as described above.

Quantitative RT-PCR. Total cellular RNA was isolated using the RNA Mini Kit (QIAGEN). Total RNA from tumors was isolated using Trizol (Invitrogen) according to the manufacturer's instructions. An RT-PCR kit (PE Biosystems) and 1 μg of total RNA were used to perform RT-PCR according to the manufacturer's instructions. Real-time PCR was performed using an ABI-Prism 7700 Sequence Detector (Applied Biosystems), as previously described (60). Human CA9 and VEGF primers have been described previously (62). Other primers are listed in Table 2. As an internal control, 18S rRNA was used. Data are expressed as fold change relative to the control sample, as previously described (60).

Immunoblotting. Western blot analysis from whole cell lysates was performed as described previously (63). The following antibodies were used: HIF-1α and p21 (BD Biosciences); HIF-2α (Novus Biologicals); β-actin (Millipore); pSTAT1 (Ser 727), pSTAT1 (Tyr 701), total STAT1, total STAT3, pSTAT3 (Ser727), pSTAT3 (Tyr705), pERK1/2, total ERK, pAKT, total AKT, and total p38 (Cell Signaling); p-p38 (Invitrogen); and p–c-Jun (Ser73) (Santa Cruz Biotechnology).

Anchorage-independent growth assay (soft agar assay). Cells cultured under normoxic or hypoxic conditions were collected and suspended in 0.4% agar containing RPMI with 5% FBS and overlaid onto a bottom layer of 0.75% agar in 6-well plates (5,000 cells per well). Colonies were counted after 13 days using the colony counter Gel Count (Oxford Optronix). Soft agar was prepared with low melting temperature agarose (Lonza) dissolved in PBS and autoclaved before use.

Clonogenic assay. Cells cultured under normoxic or hypoxic conditions for the times indicated in the figure legends were collected and plated in 60-mm dishes (500 cells per dish) in RPMI containing 5% FBS. Colonies, detected after 10 days, were air dried overnight and stained with crystal violet (Sigma-Aldrich) in 20% methanol for 1 hour. Colonies were counted using LabWorks Software (Ultra-Violet Products Ltd.).

Proliferation assay. Cells were seeded into 96-well plates at a density of 7,500 cells per well and allowed to grow for 24, 48, and 72 hours under normoxic or hypoxic conditions at 37°C in 5% CO_2. Cell viability was then assessed with a sulforhodamine B assay as previously described (64) and read on SpectraMax 190 plate reader at 515 nm (Molecular Devices).

Flow cytometry. To evaluate cell surface expression of IL-11Rα, cells were stained with specific PE-conjugated antibodies (Santa Cruz Biotechnology) and analyzed using flow cytometry (FACScan; BD). Samples were gated on a dot plot showing forward scatter and side scatter in order to exclude cell debris not within normal cell size. Gated cells were plotted on a histogram plot showing the background staining overlay with the sample staining. Annexin V staining was performed using the annexin V fluorescein isothiocyanate apoptosis kit (BD Biosciences) according to the manufacturer's instructions. Determination of cell cycle distribution was performed using Guava Cell Cycle Reagent (Millipore) according to the manufacturer's instructions.

CHIP assay/re-CHIP. ChIP-IT Express and Re-ChIP–IT were purchased from ActiveMotif. ChIP/Re-ChIP was conducted according to the manufacturer's protocol. Anti–HIF-1α monoclonal antibody was from Novus Biologicals, and anti–c-Fos polyclonal antibody was from

Table 2
Quantitative RT-PCR primers

Gene	Primer	Sequences
Human *IL11*	Forward	5′-TCTCTCCTGGCGGACACG-3′
	Reverse	5′-AATCCAGGTTGTGGTCCCC-3′
Human *IL6*	Forward	5′-CAATCTGGATTCAATGAGGAGAC-3′
	Reverse	5′-CTCTGGCTTGTTCCTCACTACTC-3′

Table 3
ChIP assay/re-ChIP primers

Gene	Primer	Sequence
***VEGF* promoter containing HRE**	Forward	5′-CCTTTGGGTTTTGCCAGA-3′
	Reverse	5′-CCAAGTTTGTGGAGGCTGA-3′
Cyclin D1 promoter	Forward	5′-CTACACCCCCAACAAAACCA-3′
	Reverse	5′-TAACCGGGAGAAACACACCT-3′
***IL11* promoter**	Forward	5′-AGCCTGAGTGTCTGCTCCG-3′
	Reverse	5′-TGACACATCCTGACTCACCCTCC-3′
***VEGF* promoter containing AP1 site**	Forward	5′-GCAGCTGGCCTACCTACCTT-3′
	Reverse	5′-ACTGAGAACGGGAAGTGGAG-3′

Santa Cruz Biotechnology Inc. For immunoprecipitation, 2 μg of each corresponding antibody were used. PCR primer sets can be found in Table 3. Primer concentration was 10 pmol/20 μl for each PCR reaction. The PCR products were run on a 3.0% agarose gel after 32–35 cycles and analyzed using ethidium bromide.

IL-11 ELISA. Total levels of IL-11 protein were measured on supernatants using the human IL-11 Quantikine ELISA kit (R&D Systems) according to the manufacturer's instructions. Levels of IL-11 protein were normalized to the total amount of protein in each sample.

Animal studies. Studies were conducted in an Association for Assessment and Accreditation of Laboratory Animal Care International–accredited (AAALAC-accredited) facility with an approved animal protocol (NIH Institutional Review Board). PC3 cells (1×10^7) stably expressing shRNA targeting either luciferase (NC) or IL-11KD (#1 or #2) were injected s.c. into the flank of female athymic nude (NCr/nu) mice (Animal Production Area, Frederick National Laboratory for Cancer Research). Tumor size was determined by collecting length and width measurements and calculating the tumor weight (mg) as [tumor length × (tumor width)^2] / 2. When mice were sacrificed, tumors from each animal were harvested and used for histopathological studies and to analyze mRNA.

Immunohistochemistry. Tumors were fixed in 4% paraformaldehyde and embedded in paraffin. Monoclonal anti-CD43 (RAM34) antibody was used at a dilution of 1:100 (Santa Cruz Biotechnology). Polyclonal rabbit anti-Ki67 antibody was used at a dilution of 1:10,000. TUNEL staining was performed using the ApopTag kit from Millipore, according to the manufacturer's instructions. Detection was done using standard avidin-biotin complex methods. Images were captured using a Retiga 2000R CCD camera outfitted with an RGB filter (Qimaging) on a Nikon Eclipse 80i upright microscope. All images were captured under consistent illumination and exposure for their respective stains. CD34, Ki67, ApopTag, and H&E staining were imaged using ×20 (Nikon Plan Apo; numerical aperture: 0.75) and ×40 (Nikon Plan UW; numerical aperture: 0.06) objectives. For CD34, ApopTag, and Ki67 analysis, 10 fields per sample were pseudo-randomly selected. Slides were scanned using a Scanscope CS (Aperio) at ×20 and ×40 magnification using default system settings. Images were extracted using Imagescope. No image postprocessing was done to enhance or alter the original images. Image analysis was conducted through Image-Pro Plus v6.1 (MediaCybernetics). Custom-made scripts were developed to analyze the respective target signals using various color and morphological segmentation tools. Post-capture image modification was limited to contrast enhancement.

Statistics. All data were analyzed with Microsoft Excel using a t test assuming equal variances or GraphPad Prism 4 (GraphPad Software) and the Mann-Whitney nonparametric *t* test. The results of the in vivo experiments were tested for outliers using Grubb's test (GraphPad Software). A *P* value of less than 0.05 was considered statistically significant, and is indicated as such in figure legends.

Microarray. HCT116 colon cancer cells were serum starved and exposed to hypoxia (1% O_2) or normoxia (21% O_2) for 3 days. Microarray analysis was performed using Affymetrix arrays (HG-U133 Plus 2.0). Data were deposited into Gene Expression Omnibus (GEO; http://www.ncbi.nlm.nih.gov/geo/), which is a Minimum Information About a Microarray Experiment–compliant (MIAME-compliant) public database; the accession number is GSE43608.

Study approval. The Frederick National Laboratory for Cancer Research is accredited by AAALAC and follows the Public Health Service Policy on the Care and Use of Laboratory Animals. Animal care was provided in accordance with the procedures outlined in the Guide for Care and Use of Laboratory Animals (65). Studies were conducted in female athymic nude (NCr/nu) mice obtained from the Animal Production Area (Frederick National Laboratory for Cancer Research) in an AAALAC-accredited facility, following an approved animal protocol (NIH Institutional Review Board).

Acknowledgments

The authors thank Miriam Anver for analysis of immunohistochemistry slides, Beverly Teicher for critical review, and Badarch Uranchimeg for technical support. This project was funded by federal funds from the National Cancer Institute (NIH contract HHSN261200800001E) and by the Developmental Therapeutics Program in the Division of Cancer Treatment and Diagnosis of the National Cancer Institute. The content of this publication does not necessarily reflect the views or policies of the Department of Health and Human Services, nor does mention of trade names, commercial products, or organizations imply endorsement by the US Government.

Received for publication June 21, 2011, and accepted in revised form January 24, 2013.

Address correspondence to: Giovanni Melillo, Discovery Medicine-Oncology, Bristol-Myers Squibb, Route 206 and Province Line Rd., Princeton, New Jersey 08540, USA. Phone: 609.252.6975; Fax: 609.252.7821; E-mail: giovanni.melillo@bms.com. Or to: Annamaria Rapisarda, Tumor Microenvironment Laboratory/Molecular Pharmacology Branch/DTP, Frederick National Laboratory for Cancer Research, SAIC-Frederick Inc., PO Box B, Frederick, Maryland 21702, USA. Phone: 301.846.5050; Fax: 301.846.6081; E-mail: rapisardaa@mail.nih.gov.

1. Harris AL. Hypoxia — a key regulatory factor in tumour growth. *Nat Rev Cancer*. 2002;2(1):38–47.
2. Semenza GL. Hypoxia and cancer. *Cancer Metastasis Rev*. 2007;26(2):223–224.
3. Graeber TG, et al. Hypoxia-mediated selection of cells with diminished apoptotic potential in solid tumours. *Nature*. 1996;379(6560):88–91.
4. Huang LE, Bindra RS, Glazer PM, Harris AL. Hypoxia-induced genetic instability — a calculated mechanism underlying tumor progression. *J Mol Med*. 2007;85(2):139–148.
5. Rapisarda A, Melillo G. Role of the hypoxic tumor microenvironment in the resistance to anti-angiogenic therapies. *Drug Resist Updat*. 2009;12(3):74–80.
6. Brown JM, Wilson WR. Exploiting tumour hypoxia in cancer treatment. *Nat Rev Cancer*. 2004;4(6):437–447.
7. Melillo G. Targeting hypoxia cell signaling for cancer therapy. *Cancer Metastasis Rev*. 2007;26(2):341–352.
8. Wang GL, Jiang BH, Rue EA, Semenza GL. Hypoxia-inducible factor 1 is a basic-helix-loop-helix-PAS heterodimer regulated by cellular O2 tension. *Proc Natl Acad Sci U S A*. 1995;92(12):5510–5514.
9. Zhong H, et al. Overexpression of hypoxia-inducible factor 1alpha in common human cancers and their metastases. *Cancer Res*. 1999;59(22):5830–5835.
10. Birner P, Schindl M, Obermair A, Breitenecker G, Oberhuber G. Expression of hypoxia-inducible factor 1alpha in epithelial ovarian tumors: its impact on prognosis and on response to chemotherapy. *Clin Cancer Res*. 2001;7(6):1661–1668.
11. Birner P, Schindl M, Obermair A, Plank C, Breitenecker G, Oberhuber G. Overexpression of hypoxia-inducible factor 1alpha is a marker for an unfavorable prognosis in early-stage invasive cervical cancer. *Cancer Res*. 2000;60(17):4693–4696.
12. Aebersold DM, et al. Expression of hypoxia-inducible factor-1alpha: a novel predictive and prognostic parameter in the radiotherapy of oropharyngeal cancer. *Cancer Res*. 2001;61(7):2911–2916.
13. Bos R, et al. Levels of hypoxia-inducible factor-1alpha independently predict prognosis in patients with lymph node negative breast carcinoma. *Cancer*. 2003;97(6):1573–1581.
14. Taga T, Kishimoto T. Gp130 and the interleukin-6 family of cytokines. *Annu Rev Immunol*. 1997;15:797–819.
15. Yin T, Yang YC. Mitogen-activated protein kinases and ribosomal S6 protein kinases are involved in signaling pathways shared by interleukin-11, interleukin-6, leukemia inhibitory factor, and oncostatin M in mouse 3T3-L1 cells. *J Biol Chem*. 1994;269(5):3731–3738.
16. Fuhrer DK, Yang YC. Complex formation of JAK2 with PP2A, P13K, and Yes in response to the hematopoietic cytokine interleukin-11. *Biochem Biophys Res Commun*. 1996;224(2):289–296.
17. Fuhrer DK, Yang YC. Activation of Src-family protein tyrosine kinases and phosphatidylinositol 3-kinase in 3T3-L1 mouse preadipocytes by interleukin-11. *Exp Hematol*. 1996;24(2):195–203.
18. Paul SR, et al. Molecular cloning of a cDNA encoding interleukin 11, a stromal cell-derived lymphopoietic and hematopoietic cytokine. *Proc Natl Acad Sci U S A*. 1990;87(19):7512–7516.
19. Weich NS, et al. Recombinant human interleukin-11 directly promotes megakaryocytopoiesis in vitro. *Blood*. 1997;90(10):3893–3902.
20. Putoczki T, Ernst M. More than a sidekick: the IL-6 family cytokine IL-11 links inflammation to cancer. *J Leukoc Biol*. 2010;88(6):1109–1117.
21. Bollrath J, et al. gp130-mediated Stat3 activation in enterocytes regulates cell survival and cell-cycle progression during colitis-associated tumorigenesis. *Cancer Cell*. 2009;15(2):91–102.
22. Ernst M, et al. STAT3 and STAT1 mediate IL-11-dependent and inflammation-associated gastric tumorigenesis in gp130 receptor mutant mice. *J Clin Invest*. 2008;118(5):1727–1738.
23. Xiang ZL, Zeng ZC, Fan J, Tang ZY, Zeng HY. Expression of connective tissue growth factor and interleukin-11 in intratumoral tissue is associated with poor survival after curative resection of hepatocellular carcinoma. *Mol Biol Rep*. 2012;39(5):6001–6006.
24. Necula LG, et al. IL-6 and IL-11 as markers for tumor aggressiveness and prognosis in gastric adenocarcinoma patients without mutations in Gp130 subunits. *J Gastrointestin Liver Dis*. 2012;21(1):23–29.
25. Casimiro S, et al. Analysis of a bone metastasis gene expression signature in patients with bone metastasis from solid tumors. *Clin Exp Metastasis*. 2012;29(2):155–164.
26. Gupta J, Robbins J, Jilling T, Seth P. TGFbeta-dependent induction of interleukin-11 and interleukin-8 involves SMAD and p38 MAPK pathways in breast tumor models with varied bone metastases potential. *Cancer Biol Ther*. 2011;11(3):311–316.
27. Lay V, Yap J, Sonderegger S, Dimitriadis E. Interleukin 11 regulates endometrial cancer cell adhesion and migration via STAT3. *Int J Oncol*. 2012;41(2):759–764.
28. Li TM, Wu CM, Huang HC, Chou PC, Fong YC, Tang CH. Interleukin-11 increases cell motility and up-regulates intercellular adhesion molecule-1 expression in human chondrosarcoma cells. *J Cell Biochem*. 2012;113(11):3353–3362.
29. Tang W, Yang L, Yang YC, Leng SX, Elias JA. Transforming growth factor-beta stimulates interleukin-11 transcription via complex activating protein-1-dependent pathways. *J Biol Chem*. 1998;273(10):5506–5513.
30. Campbell CL, Jiang Z, Savarese DM, Savarese TM. Increased expression of the interleukin-11 receptor and evidence of STAT3 activation in prostate carcinoma. *Am J Pathol*. 2001;158(1):25–32.
31. Campbell CL, Guardiani R, Ollari C, Nelson BE, Quesenberry PJ, Savarese TM. Interleukin-11 receptor expression in primary ovarian carcinomas. *Gynecol Oncol*. 2001;80(2):121–127.
32. Nakayama T, et al. Expression of interleukin-11 (IL-11) and IL-11 receptor alpha in human gastric carcinoma and IL-11 upregulates the invasive activity of human gastric carcinoma cells. *Int J Oncol*. 2007;30(4):825–833.
33. Yoshizaki A, Nakayama T, Yamazumi K, Yakata Y, Taba M, Sekine I. Expression of interleukin (IL)-11 and IL-11 receptor in human colorectal adenocarcinoma: IL-11 up-regulation of the invasive and proliferative activity of human colorectal carcinoma cells. *Int J Oncol*. 2006;29(4):869–876.
34. Zurita AJ, Troncoso P, Cardo-Vila M, Logothetis CJ, Pasqualini R, Arap W. Combinatorial screenings in patients: the interleukin-11 receptor alpha as a candidate target in the progression of human prostate cancer. *Cancer Res*. 2004;64(2):435–439.
35. Lacroix M, Siwek B, Marie PJ, Body JJ. Production and regulation of interleukin-11 by breast cancer cells. *Cancer Lett*. 1998;127(1–2):29–35.
36. Hanavadi S, Martin TA, Watkins G, Mansel RE, Jiang WG. Expression of interleukin 11 and its receptor and their prognostic value in human breast cancer. *Ann Surg Oncol*. 2006;13(6):802–808.
37. Lewis VO, et al. The interleukin-11 receptor alpha as a candidate ligand-directed target in osteosarcoma: consistent data from cell lines, orthotopic models, and human tumor samples. *Cancer Res*. 2009;69(5):1995–1999.
38. Yamazumi K, et al. Expression of interleukin-11 and interleukin-11 receptor alpha in human colorectal adenocarcinoma; immunohistochemical analyses and correlation with clinicopathological factors. *World J Gastroenterol*. 2006;12(2):317–321.
39. Deutscher N, et al. Functional expression of the interleukin-11 receptor alpha-chain in normal colonic epithelium and colon cancer. *Int J Colorectal Dis*. 2006;21(6):573–581.
40. Kawashima I, Takiguchi Y. Interleukin-11: a novel stroma-derived cytokine. *Prog Growth Factor Res*. 1992;4(3):191–206.
41. Bellone G, et al. Cytokine expression profile in human pancreatic carcinoma cells and in surgical specimens: implications for survival. *Cancer Immunol Immunother*. 2006;55(6):684–698.
42. Meng L, Zhou J, Sasano H, Suzuki T, Zeitoun KM, Bulun SE. Tumor necrosis factor alpha and interleukin 11 secreted by malignant breast epithelial cells inhibit adipocyte differentiation by selectively down-regulating CCAAT/enhancer binding protein alpha and peroxisome proliferator-activated receptor gamma: mechanism of desmoplastic reaction. *Cancer Res*. 2001;61(5):2250–2255.
43. Sales KJ, et al. Interleukin-11 in endometrial adenocarcinoma is regulated by prostaglandin F2alpha-F-prostanoid receptor interaction via the calcium-calcineurin-nuclear factor of activated T cells pathway and negatively regulated by the regulator of calcineurin-1. *Am J Pathol*. 2010;176(1):435–445.
44. Raval RR, et al. Contrasting properties of hypoxia-inducible factor 1 (HIF-1) and HIF-2 in von Hippel-Lindau-associated renal cell carcinoma. *Mol Cell Biol*. 2005;25(13):5675–5686.
45. Kondo K, Klco J, Nakamura E, Lechpammer M, Kaelin WG. Inhibition of HIF is necessary for tumor suppression by the von Hippel-Lindau protein. *Cancer Cell*. 2002;1(3):237–246.
46. Lee HT, et al. Interleukin-11 protects against renal ischemia and reperfusion injury. *Am J Physiol Renal Physiol*. 2012;303(8):F1216–F1224.
47. Bamba S, Andoh A, Yasui H, Makino J, Kim S, Fujiyama Y. Regulation of IL-11 expression in intestinal myofibroblasts: role of c-Jun AP-1- and MAPK-dependent pathways. *Am J Physiol Gastrointest Liver Physiol*. 2003;285(3):G529–G538.
48. Kang Y, et al. Breast cancer bone metastasis mediated by the Smad tumor suppressor pathway. *Proc Natl Acad Sci U S A*. 2005;102(39):13909–13914.
49. Laderoute KR, et al. The response of c-jun/AP-1 to chronic hypoxia is hypoxia-inducible factor 1 alpha dependent. *Mol Cell Biol*. 2002;22(8):2515–2523.
50. Laderoute KR. The interaction between HIF-1 and AP-1 transcription factors in response to low oxygen. *Semin Cell Dev Biol*. 2005;16(4–5):502–513.
51. Salnikow K, et al. The regulation of hypoxic genes by calcium involves c-Jun/AP-1, which cooperates with hypoxia-inducible factor 1 in response to hypoxia. *Mol Cell Biol*. 2002;22(6):1734–1741.
52. Koshiji M, Kageyama Y, Pete EA, Horikawa I, Barrett JC, Huang LE. HIF-1alpha induces cell cycle arrest by functionally counteracting Myc. *EMBO J*. 2004;23(9):1949–1956.
53. Kharaziha P, et al. Targeting of distinct signaling cascades and cancer-associated fibroblasts define the efficacy of Sorafenib against prostate cancer cells. *Cell Death Dis*. 2012;3:e262.
54. Heo JY, et al. Embelin suppresses STAT3 signaling, proliferation, and survival of multiple myeloma via the protein tyrosine phosphatase PTEN. *Cancer Lett*. 2011;308(1):71–80.
55. Yuan ZL, Guan YJ, Chatterjee D, Chin YE. Stat3 dimerization regulated by reversible acetylation of a single lysine residue. *Science*. 2005;307(5707):269–273.
56. Clark J, et al. Genome-wide screening for complete genetic loss in prostate cancer by comparative hybridization onto cDNA microarrays. *Oncogene*. 2003;22(8):1247–1252.
57. Mora LB, et al. Constitutive activation of Stat3 in human prostate tumors and cell lines: direct inhibition of Stat3 signaling induces apoptosis of prostate cancer cells. *Cancer Res*. 2002;62(22):6659–6666.
58. Wen Z, Zhong Z, Darnell JE. Maximal activation of transcription by Stat1 and Stat3 requires both tyrosine and serine phosphorylation. *Cell*.

1995;82(2):241–250.
59. Yu H, Pardoll D, Jove R. STATs in cancer inflammation and immunity: a leading role for STAT3. *Nat Rev Cancer*. 2009;9(11):798–809.
60. Rapisarda A, et al. Identification of small molecule inhibitors of hypoxia-inducible factor 1 transcriptional activation pathway. *Cancer Res*. 2002;62(15):4316–4324.
61. Yan Q, Bartz S, Mao M, Li L, Kaelin WG. The hypoxia-inducible factor 2alpha N-terminal and C-terminal transactivation domains cooperate to promote renal tumorigenesis in vivo. *Mol Cell Biol*. 2007;27(6):2092–2102.
62. Terzuoli E, et al. Aminoflavone, a ligand of the aryl hydrocarbon receptor, inhibits HIF-1alpha expression in an AhR-independent fashion. *Cancer Res*. 2010;70(17):6837–6848.
63. Rapisarda A, et al. Schedule-dependent inhibition of hypoxia-inducible factor-1alpha protein accumulation, angiogenesis, and tumor growth by topotecan in U251-HRE glioblastoma xenografts. *Cancer Res*. 2004;64(19):6845–6848.
64. Skehan P, et al. New colorimetric cytotoxicity assay for anticancer-drug screening. *J Natl Cancer Inst*. 1990;82(13):1107–1112.
65. National Research Council (US) Committee for the Update of the Guide for the Care and Use of Laboratory Animals, eds. *Guide for the Care and Use of Laboratory Animals*. Washington, DC: The National Academies Press; 2011.